Theor. Appl. Climatol. 80, 81–89 (2005)
DOI 10.1007/s00704-004-0092-1

Theoretical and Applied Climatology
Printed in Austria

[1] University of Bayreuth, Department of Micrometeorology, Bayreuth, Germany
[2] Institute for Atmospheric and Climate Sciences, ETH Zürich, Switzerland

Special characteristics of the temperature structure near the surface

H. Sodemann[1,2] and **Th. Foken**[1]

With 4 Figures

Received October 27, 2003; accepted June 23, 2004
Published online November 17, 2004

Summary

Detailed analyses of air temperature profiles measured over the Antarctic shelf ice revealed the frequent presence of an inversion layer in the lower 2 m above ground. The regular character of the phenomenon allowed for an in-depth description of its diurnal evolution and long-term behavior. From additional high-resolution temperature profile measurements it was observed that the inversion layer leads to a decoupling of the surface layer heat fluxes from the radiative surface temperature. It is demonstrated that bulk parameterizations are not able to provide valid predictions of turbulent heat fluxes under such conditions. A model with a three-layer temperature profile is shown to give useful estimates for the aerodynamic temperature, even in the presence of an inversion layer near the surface. This indicates a possible approach to address the limitations of current bulk parameterizations for heat fluxes in high latitudes.

1. Introduction

Measured profiles of wind and temperature in the atmospheric surface layer can usually be described by the similarity theory of Monin and Obukhov (1954; henceforth referred to as MO). In some cases however, in particular for small wind velocities and stable stratification, the near-ground temperature structure in the atmospheric surface layer has been shown to disagree with MO theory. One example are thermal internal boundary layers, which can be either due to step changes in surface temperature (Garratt, 1990), or caused by transitions in the lower section of the stability profile during the afternoon transition (Foken, 2003a; Raynor et al., 1975). Another example are counter gradient fluxes, i.e. fluxes which are not in agreement with the mean gradient. Counter gradient heat fluxes are probably related to coherent structures and have so far mostly been investigated over tall vegetation (Denmead and Bradley, 1985).

Similar features not in agreement with MO similarity theory have also been observed in temperature profiles measured over smooth surfaces. However, these peculiarities could not be explained by the mechanisms described above. Over the Black Sea, an inversion layer has been reported which was situated directly above the water surface (Andreev et al., 1969; Chundshua and Andreev, 1980). Heat release from chemical reactions involving aerosols were assumed as a cause for this phenomenon. A similar observation has been made over the Caspian Sea (Foken and Kuznecov, 1978; Foken, 2003b). In the latter case, the feature was named ‘condensation layer’, as heat release from condensation processes was proposed as a possible formation mechanism. In the literature, there are still few

studies about such phenomena in the temperature structure of the surface layer, and up to now no comprehensive interpretation of these observations exists. This is partly due to their rare occurrence, partly due to the fact that skepticism against the experimental results may sometimes have hindered more thorough research.

This work presents a detailed investigation of near-surface inversion phenomena in the temperature structure above a snow surface in stable stratification. Measurements took place during the FINTUREX 1994 campaign on the Antarctic ice shelf (Foken, 1996; Handorf et al., 1999). Besides examining the temporal and structural characteristics of the temperature profile in the lowest 2 m above ground, the longer-term behavior of the stability structure in the surface layer is investigated. Furthermore, the consequences that these phenomena have for turbulent heat flux measurements and bulk models predictions are examined. Finally, this study assesses the capability of a three-layer model for the temperature profile (Foken, 1984) to provide an estimate for the aerodynamic temperature when an inversion layer is present near the surface.

2. The FINTUREX experiment

The FINTUREX campaign took place from 18 January to 19 February 1994 at Neumayer station (70°39′ S, 8°15′ W), Antarctica. The station is situated on the Ekström Ice Shelf at 42 m above sea level. The surface of the Ekström Ice Shelf is flat and homogeneous with a gentle slope of less than 0.001 from SSW to NNE. Profiles of wind velocity and temperature were acquired using a profile tower with various measurement heights between 0.5 m and 12 m (Table 1). Several measurements with a drop sonde (Foken, 1975) provided snapshots of the vertical fine structure of the air temperature profile for selected situations. The drop sonde was equipped with a platinum resistance sensor with a diameter of 2 µm and a length of 1 mm; the dropping velocity of the sonde was $1\,\mathrm{m\,s^{-1}}$. Furthermore, fluctuations of the components of the wind vector and of temperature were measured at three levels using sonic anemometers. Specific humidity fluctuations were measured at two levels by means of Lyman-α-hygrometers. Additional temperature fluctuation data was acquired using thin Pt-wire fast-response sensors. Radiative surface temperature was obtained from outgoing long-wave radiation using an IR thermometer, and assuming an emissivity of $\varepsilon = 0.96$ for the aged snow surface.

Typical errors of the profile measurements were about $0.1\,\mathrm{m\,s^{-1}}$ for the anemometers, 0.1 K for the air temperature sensors, and 0.5 K for the radiative surface temperature. The wind and temperature profile data were interpolated to 0.2 m resolution using a smoothed spline-fitting algorithm (Akima, 1970; Handorf et al., 1999). At high wind speeds, snow drift disturbed the drop sonde measurements, while below $1\,\mathrm{m\,s^{-1}}$ no dynamically induced molecular sublayer was present near the ground. The available drop sonde profiles are generally in agreement with the temperature profiles from the 12 m tower. All fluctuation measurements were performed with a sampling rate of 20 Hz. The sonic anemometers were adjusted vertically and rotated automatically into the mean wind direction. Since the terrain had a very small inclination, no transformation of the vertical coordinate was required to make $\bar{w} = 0.0\,\mathrm{m\,s^{-1}}$. Several quality

Table 1. Instrumentation of the FINTUREX campaign 1994 (Handorf et al., 1999)

Meteorological parameter	Heights of sensors in m	Instrument
Temperature fluctuations Horizontal and vertical wind fluctuations	1.7, 4.2, 11.6	Kaijo–Denki sonic anemometer, Probe A, DAT-310
Temperature fluctuations Humidity fluctuations	1.7, 4.2	15 µm Pt-wires Lyman-α-hygrometer
Temperature	0.5, 1, 2, 4.5, 10	Psychrometer, ventilated and radiation-shielded
Wind speed	0.5, 1, 2, 3.1, 4.5, 6, 8, 10	Cup anemometer

tests were regularly applied to the data, including controls of steady state flow conditions and intermittent turbulence (Foken and Wichura, 1996). The uncertainty of the friction velocity u_* was of the order of 5% to 10% for values larger than $0.1\,\mathrm{m\,s^{-1}}$. For the sensible and the latent heat fluxes, however, the uncertainty increased to 20% or even 50% due to their small magnitude. Since absolute humidity was low, differences between the sensible heat fluxes derived from the fast response temperature sensors and the buoyancy flux measured with the sonic anemometer-thermometer were small. Furthermore, no WPL correction (Liebethal and Foken, 2003; Webb et al., 1980) was necessary, as both sensible heat fluxes and specific humidity were small.

3. Temperature and stability structure

The available drop sonde profiles allowed for a direct observation of the high-resolution temperature structure in the surface layer. Two such high-resolution temperature profiles measured within one hour on 13 February 1994 show a cooling for the upper part of the profile, whereas a warming occurred in the lower part (Fig. 1). In this case, the lower part (below 0.5 m) of the surface layer temperature profile became thermally decoupled from the layers above, i.e. the temperature gradient in the decoupled layer below did not reflect the heat fluxes measured within the surface layer. The same separated behavior was observable in the interpolated temperature profiles from the 12 m tower, albeit at lower spatial resolution.

The only observable cause for these changes in the profiles was an increase in altocumulus cloudiness from 6/8 to 8/8 between the two observations, decreasing the outgoing long-wave radiation. Accordingly, both IR surface temperature and the air temperature below 0.5 m reacted with an increase to the changed radiation balance, while the air temperature above 0.5 m experienced ongoing radiative cooling. In other cases (not shown), the radiative surface temperature became even higher than the air temperature at 0.5 m, again coinciding with changes in cloud cover. Even for increases in cirrus cloudiness the outgoing long-wave radiation could be modified sufficiently to show reduced cooling in the decoupled layer. Hence, in such situations heat fluxes in the surface layer become decoupled from the temperature near the surface, and the aerodynamic temperature can no longer be assumed to be identical with the snow surface temperature (Mahrt and Vickers, 2003). Consequently, bulk models using the IR surface temperature will in these cases not be able to provide reliable predictions for turbulent heat fluxes in the surface layer.

The reason for the decoupling between surface temperature and heat fluxes was the presence of a stable inversion layer in the lower 1.5 m of the

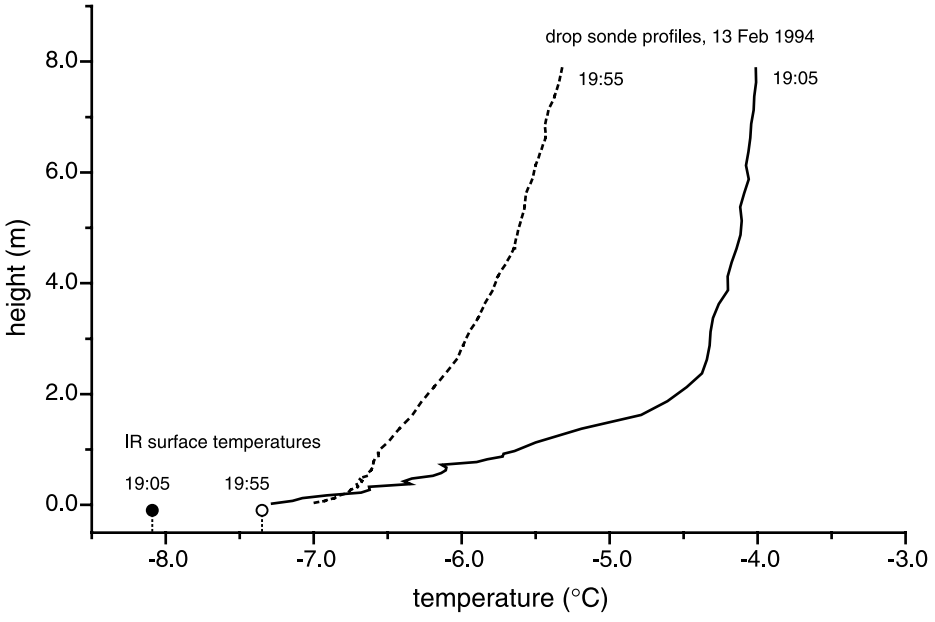

Fig. 1. Temperature structure over the snow surface during evening cooling on 13 Feb 1994, measured with a drop sonde during the FINTUREX campaign (times in UTC). Circles mark the respective IR surface temperatures. Note the temperature decrease in the upper part of the profile along with the increase in the air temperature in the lower section during the evening transition

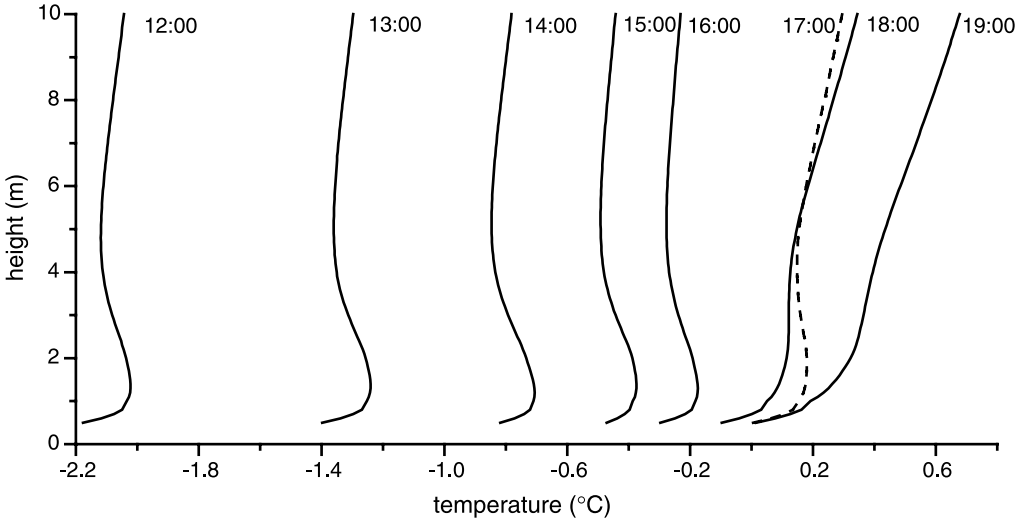

Fig. 2. Evolution of the temperature profile in the surface layer in the afternoon of 31 Jan 1994 (times in UTC). Consecutive temperature profiles are offset by 0.4 K each. For clarity, the profile at 17:00 is drawn as a dashed line

temperature profile (Fig. 1, profile at 19:05). This near-surface inversion was a regular feature in the lowermost 1.6–1.0 m of the daytime temperature profiles during the FINTUREX campaign when wind velocities were low. A typical sequence of the evolution of this inversion layer begins at noon, when the temperature difference between the near-surface inversion layer and the layers above is most developed (Fig. 2). During the afternoon, the upper part of the profile progressively recedes towards a logarithmic shape due to radiative cooling, while a stable profile is maintained in the lower profile section throughout the day. In the morning period, the evolution of the temperature profile advances in the opposite direction. When an inversion layer was present, air temperature differences between the inversion layer and adjacent layers could reach up to 0.2 K. These characteristics of the near-surface inversion layer above the Antarctic shelf ice show structural similarities with the inversion layers observed previously above the sea surface (Andreev et al., 1969; Chundshua and Andreev, 1980; Foken and Kuznecov, 1978).

Three observations confirm that the near-surface inversion layer is not a measurement artifact. Firstly, normal logarithmic temperature profiles occurred occasionally during the course of the day, which would not be the case if there was a general bias in the temperature measurements. Secondly, the inversion layer was absent during periods of higher wind shear, pointing towards an aerodynamic process at the origin of the phenomenon. And thirdly, the interpolated temperature profiles show general agreement with the independent drop sonde measurements.

The regularity of the temperature profile changes allowed for examining the long-term evolution of the stability structure in the surface layer. To this end, stability profiles were calculated from the interpolated 12 m tower measurements by means of the gradient-Richardson number Ri_G:

$$Ri_G(z) = -\frac{g}{\overline{T_L}} \frac{\partial \overline{T}/\partial z}{(\partial \overline{u}/\partial z)^2} \tag{1}$$

Thereby, g is the acceleration due to gravity, $\overline{T_L}$ is a mean layer temperature, z is the height above ground, and $\partial \overline{T}/\partial z$ and $\partial \overline{u}/\partial z$ are the temperature and wind speed gradients, respectively.

A three-layered stability structure has been reported before for the Antarctic boundary layer (Forrer and Rotach, 1997; Handorf et al., 1999). For our observations, above the stable inversion layer close to the surface (1–2 m above ground) as described above, a layer of variable stability was situated, roughly ranging from 1–2 m to 4–6 m above ground (Fig. 2). During daytime, this variable layer could exhibit near-neutral to unstable stratification, while at night it became stably stratified. Towards the top of the surface layer (above 4–6 m above ground), the variable layer merged into the permanently stable background stratification of the free atmosphere.

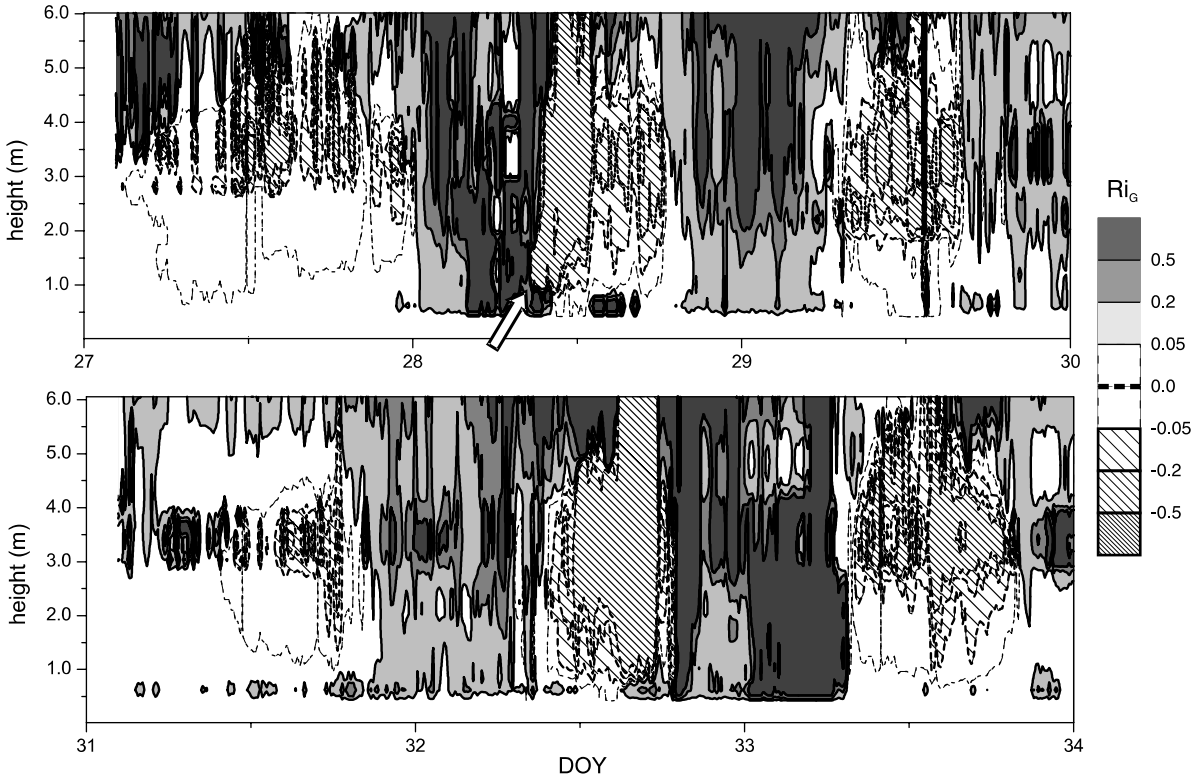

Fig. 3. Temporal development of the height profile of the gradient Richardson number (Ri_G) in the surface layer for a period of low wind velocities (27 Jan to 03 Feb 1994). The diurnal cycle creates an alternating pattern of stable (shaded) and unstable periods (hatched). The arrow marks the onset of the development of an unstable layer on top of the stable inversion layer near the surface. Note that throughout most of the period, the near-surface inversion layer can be observed in the lower 1 m above ground

Figure 3 shows the temporal evolution of the stability profile in the lower 6 m above ground for a period of predominantly katabatic winds (DOY 27–34) associated with relatively low wind velocities. After a mostly neutral period on DOY 27, wind direction changed on DOY 28, favoring stable stratification throughout the profile. At the onset of sunrise, an unstable layer developed on top of the stable near-surface inversion layer (Fig. 3, arrow). Temperature profiles in that situation are similar to the profile at 18 UTC in Fig. 2, with heat fluxes within the unstable layer decoupled from the surface temperature. Only around noon did the surface layer become fully unstable and connect to the surface. Shortly thereafter the near-surface inversion layer formed again. The same process could be observed on DOY 29, DOY 32, and less clearly on DOY 31 due to the higher wind velocities at that time. During DOY 33 stronger winds turned the whole surface layer unstable again.

The temperature profiles interpolated using the Akima (1970) smoothed spline algorithm agreed generally well with observed high-resolution temperature profiles from the available drop sonde measurements, except for too smooth transitions from the top of the near-surface inversion to the stable background stratification above. This is for example visible in the transition from 2 m to 4 m in the temperature profile at 13:00 in Fig. 2, where the actual temperature profile would exhibit a sharper transition at the top of the near-surface inversion layer (NSIL). This causes a slight underestimation of the vertical extent of the NSIL in Fig. 3. When calculating Ri_G, the too smooth transition can also result in computational noise within neutral stratification, for example visible on DOY 31 between 3.0 m and 4.0 m above ground (Fig. 3). This occasional interpolation artifact does however not affect the identification of the near-surface inversion layer.

The mere observation gives little clue about the processes behind the described phenomenon. Chemical reactions (Andreev et al., 1969; Chundshua et al., 1980), or condensation processes (Foken and Kuznecov, 1978) are unlikely to play a role here. Rather, sublimation processes at the surface or on suspended fine ice particles could be a possible cause. Another possible mechanism is the combination of an aerodynamic decoupling with radiative flux divergence. According to this hypothesis, the streamlines are optimally adapted to the wind profile for smooth surfaces within some decimeters above the snow surface carved with sastrugies. Below this level, long-wave radiative processes as opposed to influences from the wind profile dominate. As the radiation balance in the late Antarctic summer creates a long-wave cooling even at daytime, a stable layer can then persist in the lowest meter above the surface. Such a process would be similar to decoupling phenomena observed above high vegetation (Finnigan, 2000). As the developing unstable layer is not connected to the surface, other sources for the observed heat flux must be taken into consideration; either locally within the surface layer, or remotely due to advection. Yet, with the current knowledge, no definite explanation for the observed characteristics of the temperature profile can be given.

4. Surface temperature and turbulent heat fluxes

Bulk models are one of the most common approaches to calculate turbulent heat fluxes in the surface layer. The bulk formulation for the heat flux is usually written as

$$Q_H = \rho c_p C_H u(z)[T_0 - T(z)], \qquad (2)$$

where Q_H is the sensible heat flux, T_0 is the aerodynamic temperature, $T(z)$ is the air temperature, C_H is the transfer coefficient for heat, ρ is the air density, and c_p is the specific heat capacity of air. For the heights considered here, no correction for potential temperature is required. A constant value of $C_H = 1 \times 10^{-3}$ was used for the bulk model. C_H is often formulated as a function of stability and the roughness length of heat, such as in the surface layer flux parameterization of Louis (1979). However, in particular for stable stratification, this stability dependence is not well known (Handorf et al., 1999). Hence, here we applied the model as formulated for near-neutral conditions to the Antarctic surface layer and account for the consequences of this simplification during the discussion.

In models for the turbulent heat flux, the radiometric surface temperature is usually considered as equal to the aerodynamic temperature, even if they are theoretically different (Mahrt and Vickers, 2003). Experimentally, the radiometric surface temperature is measured using an IR thermometer, whereas in numerical models it can be calculated from the radiation balance at the surface. Radiative temperatures are usually larger than aerodynamic temperatures. Hence, using the radiative temperature in bulk models instead of the aerodynamic temperatures creates a bias towards larger heat fluxes for stable stratification. In the presence of a near-surface inversion layer, the assumed equality between the two temperatures becomes even more questionable and does not hold any more. This becomes obvious when comparing the predicted heat fluxes from the bulk model (Eq. 2) using IR surface temperatures with turbulent heat flux measurements at 1.7 m (Fig. 4a). The disagreement between measured and predicted heat fluxes is largest in stable stratification, i.e. when Q_H is negative. The poor performance of MO similarity theory in stable stratification has long been recognized (e.g. Handorf et al., 1999; Forrer and Rotach, 1997). To some degree the assumption of a constant C_H may have contributed to the scatter for negative heat fluxes. Yet, most of the disagreement between the heat flux predictions and the flux measurements is apparently related to the presence of the near-surface inversion layer (NSIL). For one cluster of points where the NSIL was observed, the bulk model even predicts positive heat fluxes, while the measured fluxes are strongly negative. Hence, under these circumstances, the bulk model is obviously not able to provide meaningful flux predictions.

One approach to overcome the decoupling due to a near-surface inversion layer in models is to derive a modeled surface temperature similar to the aerodynamic temperature, which is more representative for the heat fluxes in the surface layer. Such a modeled surface temperature can be estimated from a three-layer temperature profile model (Foken, 1984), which originally was

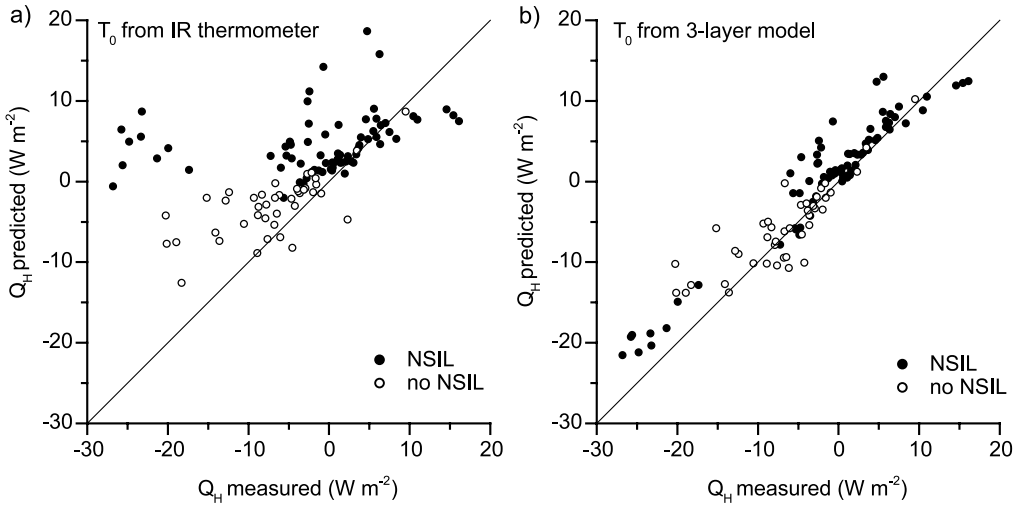

Fig. 4. Comparison of measured turbulent heat flux Q_H at 1.7 m with predictions from a bulk model using **a**) the IR surface temperature, and **b**) an estimate of the aerodynamic surface temperature from a three-layer temperature profile model. Data are classified into those where a near-surface inversion layer (NSIL) was present (full dots) and absent (open dots). The line gives the 1:1 relation between measurements and observations

intended to be used for calculating heat fluxes in the surface layer. In this model, the temperature profile in the surface layer is separated into a 1 mm thick molecular boundary layer directly at the surface, followed by a 1 cm thick buffer layer, and a turbulent layer above. The model is based on experimental work on the molecular sublayer over the ocean (Foken et al., 1978; Foken, 2002). Predicted heat fluxes from the model and experimental data were shown to agree well (Foken, 1984; 1986).

The basic idea of three-layer models is to replace the product of wind velocity and the transfer coefficient for heat in the bulk formulation (Eq. 2) by a so-called profile coefficient Γ (Bjutner, 1974; Kitajgorodskij and Volkov, 1965; Mangarella et al., 1972; 1973):

$$Q_H = \Gamma[T_0 - T(z)], \tag{3}$$

This profile coefficient Γ can be determined by integrating over the three layers:

$$\Gamma = \left(\int_0^z \frac{dz}{K_T + \nu_{Tt} + \nu_T} \right)^{-1}, \tag{4}$$

where K_T is the turbulent exchange coefficient for temperature, ν_T is the molecular temperature diffusion coefficient and ν_{Tt} is the molecular-turbulent temperature diffusion coefficient. First integrations of Γ were performed over a continuous viscous sublayer (Montgomery, 1940; Sverdrup, 1937/38). Direct measurements of the molecular temperature sublayer led to the derivation of a dimensionless thickness ${\delta_T}^+$ for this layer, which depends on the wave structure of the water surface (Foken et al., 1978):

$${\delta_T}^+ = 7.5 \cdot \frac{u_*}{\nu}[2 + \sin(\zeta - \pi/2)]. \tag{5}$$

Here, $\nu = 1.461 \times 10^{-5}\,\mathrm{m\,s^{-1}}$ is the kinematic viscosity, and the phase shift $\zeta = 0$ (π) is applied to the windward (leeward) side of the wave. From the same measurements, the parameterization ${\delta_T}^+ \approx 4$ was derived for the dimensionless temperature difference of the buffer layer normalized by the dynamic temperature scale (Foken et al., 1978; Foken, 1979; Foken, 1984). Hence, using Eq. (5) with $\zeta = 0$, and for $u_* < 0.23\,\mathrm{m\,s^{-1}}$, the profile coefficient becomes

$$\Gamma = \frac{\kappa \cdot u_*}{(\kappa \cdot \mathrm{Pr} - 1/6) \cdot {\delta_T}^+ + 5 + \ln \frac{u_* \cdot z}{30\nu}}. \tag{6}$$

Here, $\mathrm{Pr} = 0.71$ is the molecular-turbulent Prandtl number. The other coefficients in Eq. (6) are either parameterizations or derived from hydrodynamic arguments. For heights exceeding 1 m, a stability-dependent term can be added to Eq. (6), according to the MO similarity theory. Here, the universal function by Foken and Skeib (1983) was used, which is comparable to other

well-established universal functions (Högström, 1988). After estimating Γ from Eq. (6) and rearranging Eq. (3), this model provides an estimate for a modeled surface temperature similar to the aerodynamic temperature. Here, for calculating this modeled surface temperature, measurements of friction velocity and heat flux at 1.7 m above ground were used.

When the IR surface temperature is replaced in the bulk model (Eq. 2) by the new modeled surface temperature, a much better agreement between measured and predicted heat fluxes is achieved, for cases both with and without NSIL (Fig. 4b). The predictions for the cluster of points showing large discrepancies between measurements and predictions in Fig. 4a have improved considerably as well. As for radiative temperature, a constant value of C_H was used for calculating the heat fluxes from the bulk model using the modeled surface temperature. Yet, the reduction of scatter in Fig. 4b in comparison to Fig. 4a is considerably larger than the remaining scatter in Fig. 4b. Hence, to a first approximation, neglecting the stability dependence of C_H seems to have only a minor influence on the result.

However, as the calculation of this modeled surface temperature involves using the heat flux measurements, predictions and observations in Fig. 4b are not independent from each other any more. The fact that heat flux measurements are required limits the applicability of the three-layer model as used here to provide a modeled surface temperature to cases when such data are available. Nonetheless, the improved correlation shows that the three-layer approach can give a good estimate for a temperature similar to the aerodynamic temperature, even in the presence of a near-surface inversion layer. Therefore, the three-layer model temperature could help to further investigate processes related to the presence of a near-surface inversion layer. A possible application could be to overcome the use of an aerodynamic temperature in bulk models which is ill-defined for complex configurations of the surface layer temperature profile in stable stratification. From that we argue that a detailed and physically more realistic representation of the temperature structure in the surface layer may have some potential for improving current bulk heat flux parameterizations.

5. Conclusions

Detailed investigations of the temperature structure in the surface layer over the Antarctic shelf ice revealed the frequent presence of a stable inversion layer in the lower 2 m above ground. A unique data set made an in-depth description of the diurnal cycle and long-term behavior of this phenomenon possible. Compared to similar features observed over the sea surface, the near-surface inversion layer over snow shows more regular characteristics. This highlights the relevance of the phenomenon from a climatic perspective.

The near-surface inversion layer was shown to lead to a decoupling of the turbulent heat fluxes from the IR surface temperature. Hence, over ice surfaces, it is possible that a thermal decoupling near the ground occurs, causing radiative and aerodynamic surface temperatures to be substantially different. Under such circumstances, bulk models fail to provide realistic predictions for turbulent heat fluxes in the surface layer.

A model based on a three-layer temperature profile is shown to be able to give meaningful estimates for a modeled surface temperature similar to the aerodynamic temperature, even in the presence of a near-surface inversion layer. Our approach using a 3-layer model to calculate a surface temperature could be useful in validating and improving bulk models in situations where an aerodynamic temperature is difficult to determine. Hence, we conclude that a more detailed and physically realistic representation of the temperature structure in the surface layer may be an option to overcome the limitations of current bulk models for turbulent heat fluxes.

Acknowledgements

The FINTUREX 1994 campaign was funded by the German Meteorological Service, Offenbach and the Alfred-Wegener Institute, Bremerhaven.

References

Akima H (1970) A new method of interpolation and smooth curve fitting based on local procedures. J Assc Comp Mach 17: 589–602

Andreev EG, Lavorko VS, Pivovarov AA, Chundshua GG (1969) O vertikalnom profile temperatury vblizi granicy rasdela more – atmosphera. Okeanalogija 9: 348–352

Bjutner EK (1974) Teoreticeskij rascet soprotivlenija morskoj poverchnosti. In: Dubov AS (ed) Processy perenosa vblizi poverchnosti razdela okean – atmosfera. Gidrometeoizdat, Leningrad, pp 66–114

Chundshua GG, Andreev EG (1980) O mechanizme formirovanija inversii temperatury v privodnoim sloe atmosfery nad morem. Dokl AN SSSR 255: 829–832

Denmead DT, Bradley EF (1985) Flux-gradient relationships in a forest canopy. In: Hutchison BA, Hicks BB (eds) The forest-atmosphere interaction. Dordrecht, Boston, London: D. Reidel Publ. Comp., pp 421–442

Finnigan J (2000) Turbulence in plant canopies. Ann Rev Fluid Mech 32: 519–571

Foken T (1975) Die Messung der Mikrostruktur der vertikalen Lufttemperaturverteilung in unmittelbarer Nähe der Grenze zwischen Wasser und Atmosphäre. Z Meteorol 25: 292–295

Foken T, Kitajgorodskij SA, Kuznecov OA (1978) On the dynamics of the molecular temperature boundary layer above the sea. Bound-Layer Meteorol 15: 289–300

Foken T, Kuznecov OA (1978) Die wichtigsten Ergebnisse der gemeinsamen Expedition "KASPEX-76" des Institutes für Ozeanologie Moskau und der Karl-Marx-Universität Leipzig. Beitr Meeresforsch 41: 41–47

Foken T (1979) Vorschlag eines verbesserten Energieaustauschmodells mit Berücksichtigung der molekularen Grenzschicht der Atmosphäre. Z Meteorol 29: 32–39

Foken T, Skeib G (1983) Profile measurements in the atmospheric near-surface layer and the use of suitable universal functions for the determination of the turbulent energy exchange. Bound-Layer Meteorol 25: 55–62

Foken T (1984) The parametrisation of the energy exchange across the air-sea interface. Dynam Atmos Oceans 8: 297–305

Foken T (1986) An operational model of the energy exchange across the air-sea interface. Z Meteorol 36: 354–359

Foken T (1996) Turbulenzexperiment zur Untersuchung stabiler Schichtungen. Ber Polarforschung 188: 74–78

Foken T, Wichura B (1996) Tools for quality assessment of surface-based flux measurements. Agric Forest Meteorol 78: 83–105

Foken T (2002) Some aspects of the viscous sublayer. Meteorol Z 11: 267–272

Foken T (2003a) Angewandte Meteorologie, Mikrometeorologische Methoden. Heidelberg: Springer, 289 pp

Foken T (2003b) Besonderheiten der Temperaturstruktur nahe der Unterlage. In: Chmielewski F-M, Foken T (eds) Beiträge zur Klima- und Meeresforschung. Eigenverlag Chmielewski & Foken, Berlin und Bayreuth, ISBN 3-00-011043-7, pp 103–112

Forrer J, Rotach MW (1997) On the turbulence structure in the stable boundary layer over the Greenland ice sheet. Bound-Layer Meteorol 85: 111–136

Garratt JR (1990) The internal boundary layer – A review. Bound-Layer Meteorol 50: 171–203

Handorf D, Foken T, Kottmeier C (1999) The stable atmospheric boundary layer over an Antarctic ice sheet. Bound-Layer Meteorol 91: 165–186

Högström U (1988) Non-dimensional wind and temperature profiles in the atmospheric surface layer: A re-evaluation. Bound-Layer Meteorol 42: 55–78

Kitajgorodskij SA, Volkov JA (1965) O rascete turbulentnych potokov tepla i vlagi v privodnom sloe atmosfery. Izv AN SSSR, Fiz Atm Okeana 1: 1317–1336

Liebethal C, Foken T (2003) On the significance of the Webb correction to fluxes. Bound-Layer Meteorol 109: 99–106

Louis JF (1979) A parametric model of vertical fluxes in the atmosphere. Bound-Layer Meteorol 17: 187–202

Mahrt L, Vickers D (2003) Bulk formulation of the surface heat flux. Bound-Layer Meteorol (in press)

Mangarella PA, Chambers AJ, Street RL, Hsu EY (1972) Laboratory and field interfacial energy and mass flux and prediction equations. J Geophys Res 77: 5870–5875

Mangarella PA, Chambers AJ, Street RL, Hsu EY (1973) Laboratory studies of evaporation and energy transfer through a wavy air-water interface. J Phys Oceanogr 3: 93–101

Monin AS, Obukhov AM (1954) Osnovnye zakonomernosti turbulentnogo peremesivanija v prizemnom sloe atmosfery. Trudy geofiz inst AN SSSR 24 (151): 163–187

Montgomery RB (1940) Observations of vertical humidity distribution above the ocean surface and their relation to evaporation. Pap Phys Oceanogr & Meteorol 7: 1–30

Raynor GS, Michael P, Brown RM, SethuRaman S (1975) Studies of atmospheric diffusion from a nearshore oceanic site. J Climate Appl Meteorol 14: 1080–1094

Sverdrup HU (1937/38) On the evaporation from the ocean. J Marine Res 1: 3–14

Webb EK, Pearman GI, Leuning R (1980) Correction of the flux measurements for density effects due to heat and water vapour transfer. Quart J Roy Meteor Soc 106: 85–100

Authors' address: Harald Sodemann* (e-mail: harald.sodemann@env.ethz.ch), Thomas Foken, University of Bayreuth, Department of Micrometeorology, Universitätsstraße 30, 95440 Bayreuth, Germany; *Present affiliation: Institute for Atmospheric and Climate Sciences, ETH Hönggerberg, 8093 Zürich, Switzerland.